# Protein Fragment Reconstitution as a Driving Force for Self-Assembling Reversible Protein Hydrogels

*Na Kong and Hongbin Li**

Dedicated to Dr. James Trotter, Professor of Chemistry at the University of British Columbia from 1962 to 1998

**Due to their potential biomedical applications, protein-based hydrogels have attracted considerable interest. Although various methods have been developed to engineer self-assembling, physically-crosslinked protein hydrogels, exploring novel driving forces to engineer such hydrogels remains challenging. Protein fragment reconstitution, also known as fragment complementation, is a self-assembling mechanism by which protein fragments can reconstitute the folded conformation of the native protein when split into two halves. Although it has been used in biophysical studies and bioassays, fragment reconstitution has not been explored for hydrogel construction. Using a small protein GL5 as a model, which is capable of fragment reconstitution to reconstitute the folded GL5 spontaneously when split into two halves, GN and GC, we demonstrate that protein fragment reconstitution is a novel driving force for engineering self-assembling reversible protein hydrogels. Fragment reconstitution between GN and GC crosslinks GN and GC-containing proteins into self-assembling reversible protein hydrogels. These novel hydrogels show temperature-dependent reversible sol-gel transition, and excellent property against erosion in water. Since many proteins can undergo fragment reconstitution, we anticipate that such fragment reconstitution may offer a general driving force for engineering protein hydrogels from a variety of proteins, and thus significantly expanding the 'toolbox' currently available in the field of biomaterials.**

## 1. Introduction

Protein hydrogels have attracted considerable interest over the last two decades due to their potential applications in a wide range of biomedical applications, including drug delivery, as artificial extracellular matricies and regenerative medicines.[1–3] Among engineered protein hydrogels, self-assembling hydrogels are of particular interest.[2,4,5] Inspired by the pioneering work of Tirrell and co-workers,[6] researchers have been developing novel strategies for engineering self-assembling protein hydrogels[4–8] To construct these self-assembling protein-based hydrogels, the most widely used technique involves the self-assembly of coiled-coil leucine zipper domains. These coiled-coil domains are basic folding motifs found in proteins, consisting of two or more $\alpha$-helices that self-assemble to form an intertwined superhelix. Using this robust assembling strategy, a wide range of protein hydrogels have been engineered, ranging from random coil sequence-based hydrogels, to hydrogels encompassing folded globular domains with diverse functions.[6–14] Other methodologies toward constructing hydrogels have been subsequently developed, including those based on heterodimeric molecular recognition between protein motifs,[5] including growth factor mediated hydrogels,[15] "Dock-and-Lock" hydrogels,[16,17] and mixing-induced two-component hydrogels.[18] Despite these progresses, strategies to construct self-assembling protein hydrogels remain rather limited, limiting the possibility toward the systematic engineering of protein hydrogel properties. Here, we present a novel approach toward engineering self-assembling protein hydrogels based on protein fragment reconstitution (also known as fragment complementation).

Previously, it was discovered that when some proteins split into two fragments, these fragments can undergo reconstitution to reconstitute the folded conformation of the native protein, either spontaneously or assisted by helper proteins that can bring the two fragments into proximity.[19–24] The small protein GB1 is a good example of such a protein that is capable of undergoing spontaneous reconstitution when split into two fragments[25–28] (**Figure 1**A). This assisted protein fragment reconstitution property has been used to develop assays to probe protein–protein interactions in vitro as well as in living cells.[23,24,29,30] Subsequently, a suite of proteins has been found to demonstrate such fragment reconstitution behavior, such as ubiquitin, dihydroforlate reductase, and green fluorescent protein.[19,20,22,29–31] Despite the wide ubiquity of proteins able to undergo fragment reconstitution and their application in bioassays, surprisingly, use of fragment reconstitution has not been

N. Kong, Prof. Dr. H. Li
Department of Chemistry
The University of British Columbia
2036 Main Mall
Vancouver, BC V6T 1Z1, Canada
E-mail: Hongbin@chem.ubc.ca

**DOI: 10.1002/adfm.201502277**

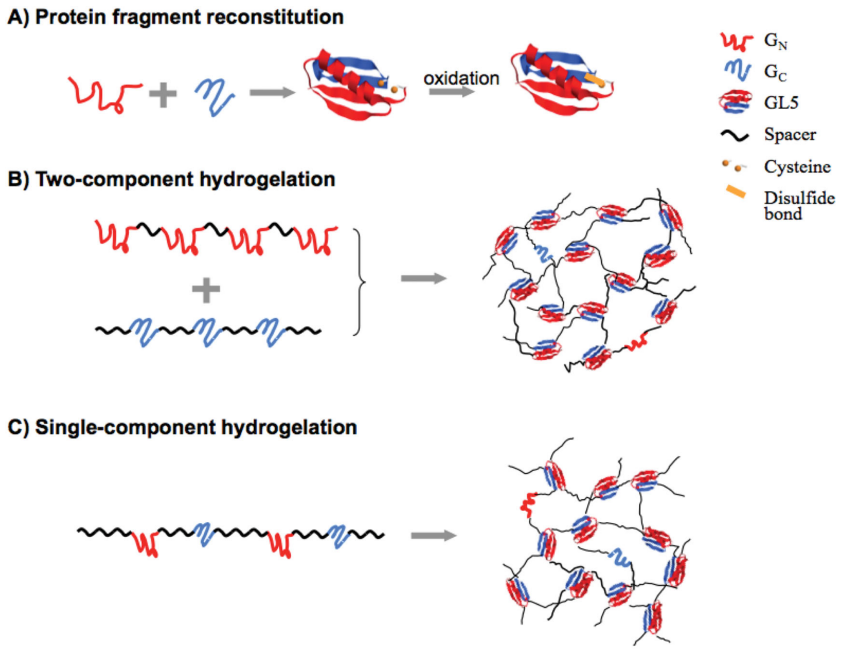


**Figure 1.** Schematic showing hydrogelation based on protein fragment reconstitution. A) Formation of reconstituted GL5 from $G_N$ and $G_C$. B) Schematic of fragment reconstitution induced two-component hydrogelation. The two tandem polyproteins, containing either $G_N$ or $G_C$ fragments, serve as multiple functional precursors for hydrogelation. C) Schematic of fragment reconstitution induced single-component hydrogelation. The tandem polyprotein, containing both $G_N$ and $G_C$ fragments, serves as a multifunctional precursor for hydrogelation.

explored in engineering self-assembling protein hydrogels or supramolecular protein polymers. For the two split fragments A and B that can undergo fragment reconstitution to reconstitute the native folded structure, it should be feasible to cross-link multifunctional polymers $(S\text{-}A)_n$ and $(S\text{-}B)_m$ into a polymer network and form a hydrogel, where S represents spacers, A and B are the two fragments capable of reconstituting, and $m$ and $n$ represent the number of repeating units (Figure 1B). Using fragments from a loop elongation variant of GB1 as a model system, we demonstrate the proof-of-principle of using protein fragment reconstitution as a driving force to engineer self-assembling protein hydrogels. Using different protein designs, we demonstrate both two-component as well as single-component approaches to engineer protein fragment reconstitution-driven protein hydrogels.

## 2. Results and Discussion

### 2.1. GL5 Can be Reconstituted via Fragment Reconstitution from Its Two Fragments $G_N$ and $G_C$

To demonstrate the concept of protein fragment reconstitution as a driving force toward engineering protein hydrogels, we used GL5 fragments as a model system. GL5 is a loop elongation variant of the small protein GB1, which has been studied extensively in protein folding studies.[32,33] It was previously shown that when GB1 is split into two fragments at residue 40, the two fragments 1–40 and 41–56 of GB1 can reassemble into a native-like fold,[25–28] with a dissociation constant $K_d$ of $\approx 9 \times 10^{-6}$ M.[27] In our previous work on mutually exclusive proteins, we found that when GL5 is split into two fragments at residue 42 (residues 1–42 and 43–61) by the insertion of a 89-residue guest domain I27, the two fragments $G_N$ (1–42) and $G_C$ (43–61) can refold to its native structure, despite the fact that $G_N$ (1–42) and $G_C$ (43–61) are separated by 89 residues.[33,34] Such refolding can be considered as intramolecular fragment reconstitution. Based on these prior studies, we reason that, if $G_N$ and $G_C$ can reconstitute into a native-like GL5 structure, fragment reconstitution between $G_N$ and $G_C$ can be used as a driving force to construct protein hydrogels.

We first carried out experiments to confirm that the two fragments $G_N$ and $G_C$ can undergo intermolecular fragment reconstitution to reconstitute the native fold of GL5. We utilized two engineered proteins $G_N$-I27w34f and I27w34f-$G_C$; for simplicity, we subsequently refer these two proteins as $G_N$-I27 and I27-$G_C$.

We performed stopped flow fluorimetry experiments using a 1:1 mixture of $G_N$-I27 and I27-$G_C$, which is similar in design to stopped flow experiments investigating the unfolding/folding kinetics of the intact GL5 domain. Since I27w34f in both $G_N$-I27 and I27-$G_C$ does not contain any tryptophan residues, any observed change in tryptophan fluorescence in stopped flow experiments should reflect the behavior of the reconstituted GL5 domain.

**Figure 2**A shows the "folding" (reconstitution) kinetics of 1:1 mixture of $G_N$-I27 and I27-$G_C$. Upon mixing at this 1:1 ratio, we observed that tryptophan fluorescence increases as a function of time in a nonlinear fashion, suggesting that some $G_N$-I27 and I27-$G_C$ reconstitute into the native fold via fragment reconstitution. In contrast, $G_N$-I27 or I27-$G_C$ alone does not show any change in tryptophan fluorescence under the same conditions. In comparison, Figure 2B shows folding kinetics of the intact GL5 domain under the same condition; the "reconstitution folding" rate of $G_N$-I27 and I27-$G_C$ is significantly slower than that of intact GL5 under similar conditions.

To further confirm the fragment reconstitution of $G_N/G_C$, we also carried out "unfolding" experiments. Figure 2C shows the "unfolding" kinetics of a 1:1 mixture of $G_N$-I27 and I27-$G_C$ (at a concentration of $10 \times 10^{-6}$ M) in 4 M GdmCl. We observed that tryptophan fluorescence shows a fast decay as a function of time, a phenomenon similar to that observed in the unfolding of intact GL5 (Figure 2D). In contrast, similar experiments on singular $G_N$-I27 or I27-$G_C$ fragments do not show any change in tryptophan fluorescence. This strongly indicates that some $G_N$-I27 and I27-$G_C$ reconstituted to the folded state, which gives rise to decaying tryptophan fluorescence under denaturing conditions. By fitting the fluorescence decay to a first-order rate equation, we measured the unfolding rate constant of the "reconstituted" $G_N/G_C$ of 18.5 $s^{-1}$ in 4 M GdmCl; this rate constant is close to the unfolding rate constant of intact GL5 under the same condition

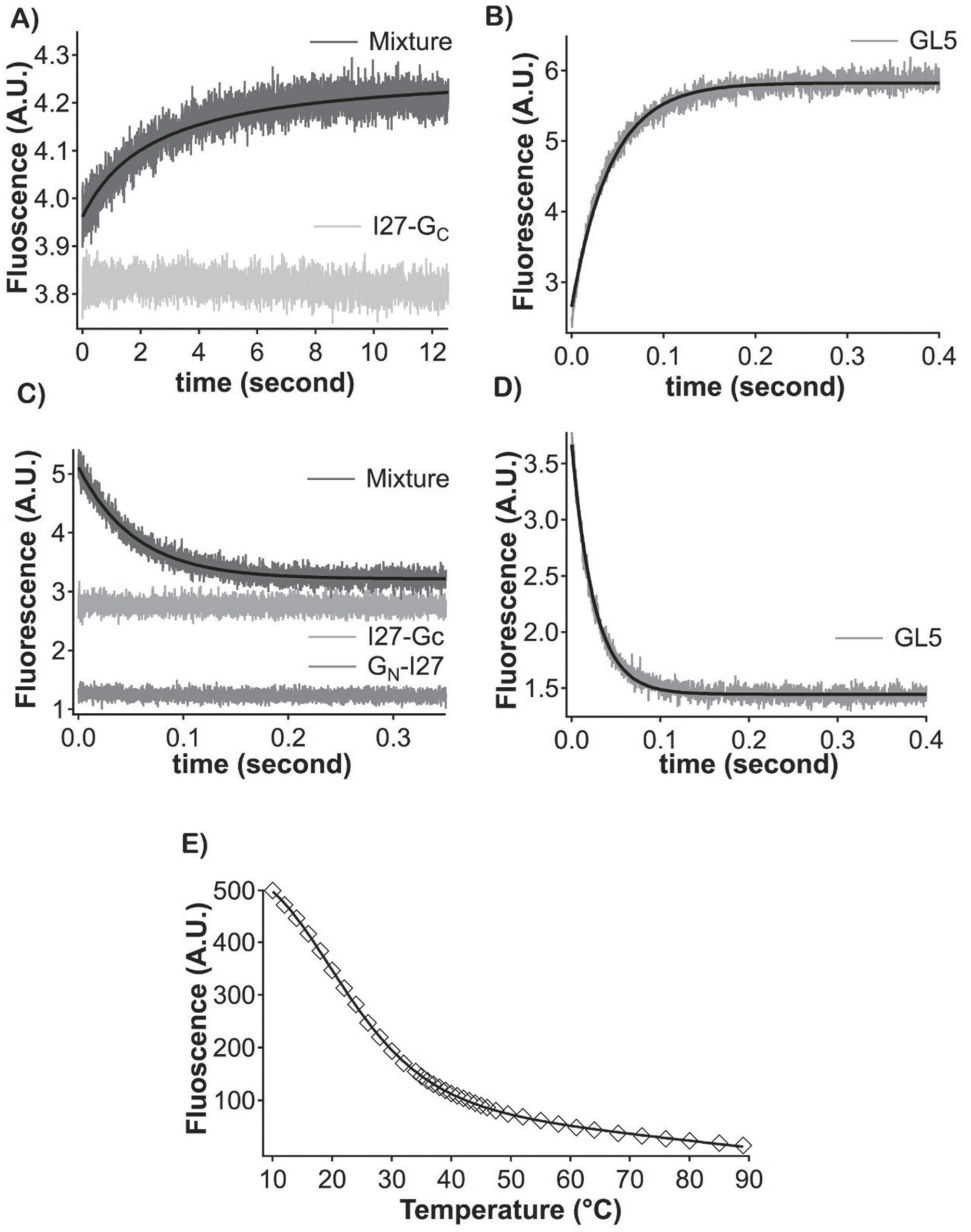


**Figure 2.** $G_N$ and $G_C$ can reconstitute into a folded structure via fragment reconstitution. A–D) Stopped-flow fluorimetry measurements of hydrogel unfolding and folding kinetics. A) Folding kinetics of a 1:1 mixture solution of I27-$G_N$ and I27-$G_C$ in PBS. The experimental data are fitted to a second-order rate law, giving a rate constant of 64 $s^{-1}$ $M^{-1}$, which is smaller than that determined by using surface plasmon resonance.[26] For comparison, the data for I27-Gc are shown. B) Refolding kinetics of GL5 in 4 M GdmCl. The rate constant was determined to be 23.6 $s^{-1}$ from a single-exponentially fit of the data. C) Unfolding kinetics of I27-$G_N$ and I27-$G_C$ mixture, I27-$G_C$ , and I27-$G_N$ in 4 M GdmCl. The solid black line shows a single-exponential fit, with an unfolding rate constant of 18.5 $s^{-1}$. D) Unfolding kinetics of GL5 in 4 M GdmCl. The black line is a single-exponential fit, with a resultant unfolding rate constant of 39.6 $s^{-1}$. E) Thermal denaturation of the I27-$G_N$ and I27-$G_C$ solution, as monitored by fluorescence. The data are fitted globally, with a $T_m$ of 22.6 °C.

(specifically, 39.6 $s^{-1}$). This close agreement supports that the observed fluorescence decay in $G_N$-I27 and I27-$G_C$ indeed results from unfolding of the reconstituted $G_N/G_C$.

This reconstituted $G_N/G_C$ has a melting temperature of 23 °C, indicating that the reconstituted $G_N/G_C$ is much less stable than intact GL5 (Figure 2E). This result is similar to previous studies on reconstituted GB1 (with a $T_m$ of 42 °C[27] for reconstituted $G_{1-40}/G_{41-56}$, and 25 °C for the reconstituted GB1 mutant GB1QDD.[25] Combined together, these results strongly indicate that $G_N$ and $G_C$ can reconstitute into a folded structure similar to the native structure of GL5 via fragment reconstitution, albeit at a lower thermodynamic stability. Thus, the reconstitution of GL5 from $G_N/G_C$ shows that it is feasible to use fragment reconstitution as a driving force to engineer self-assembling, temperature-responsive protein hydrogels.

### 2.2. Fragment Reconstitution Can Serve as a Driving Force to Design Self-Assembling Protein Hydrogels

Having confirmed that $G_N$ and $G_C$ can indeed reconstitute to form a native GB1-like fold, we then endeavored to use fragment reconstitution as a driving force toward engineering protein hydrogels. To demonstrate the feasibility of this design, we employed a two-component approach,[18,35] where two proteins $(I27\text{-}G_N\text{-}I27)_4$ and $(I27_3\text{-}G_C)_3$ were engineered and used as building blocks in hydrogel construction (Figure 1B). These two proteins can be considered as tetra- and trifunctional, where the reconstitution between $G_N$ and $G_C$ in the two proteins should result in the crosslinking of $(I27\text{-}G_N\text{-}I27)_4$ and $(I27_3\text{-}G_C)_3$, leading to the formation of a network structure when the protein concentrations are high enough. It is of note that $(I27\text{-}G_N\text{-}I27)_4$ and $(I27_3\text{-}G_C)_3$ contain different number of I27 domains, ensuring that the two proteins are not complementary in structure and will not form dimers after the association of $G_N$ and $G_C$ fragments.[10,35]

As expected, we found that mixing aqueous solutions of 10% (m/v) $(I27\text{-}G_N\text{-}I27)_4$ and 10% $(I27_3\text{-}G_C)_3$ readily leads to the formation of a transparent solid hydrogel (**Figure 3**A). By contrast, an aqueous solution of $(I27\text{-}G_N\text{-}I27)_4$ or $(I27_3\text{-}G_C)_3$ alone does not form hydrogels, even at concentrations greater than 10%. In addition, hydrogel formation involving $(I27\text{-}G_N\text{-}I27)_4$ and $(I27_3\text{-}G_C)_3$ is temperature dependent; when the temperature is greater than 23 °C (the melting temperature of the reconstituted $G_N/G_C$), $(I27\text{-}G_N\text{-}I27)_4$ and $(I27_3\text{-}G_C)_3$-based hydrogels melt into a viscous solution (Figure 3B). Upon cooling, the hydrogel can readily reform, demonstrating the reversible properties of the $(I27\text{-}G_N\text{-}I27)_4/(I27_3\text{-}G_C)_3$-based hydrogel. These results are consistent with the physical crosslinking nature of the hydrogel, which is mediated by protein fragment reconstitution. Figure 3C shows a scanning electron microscopy (SEM) micrograph of the freeze-dried 10% hydrogel, which displays an interconnected, porous network structure, with a pore size of around tens micrometers.

To characterize the mechanical properties of the hydrogel, we performed dynamic shear rheology experiments in frequency-sweep mode (Figure 3D). The storage modulus G′ of the hydrogel is ≈800 Pa, significantly larger than the loss

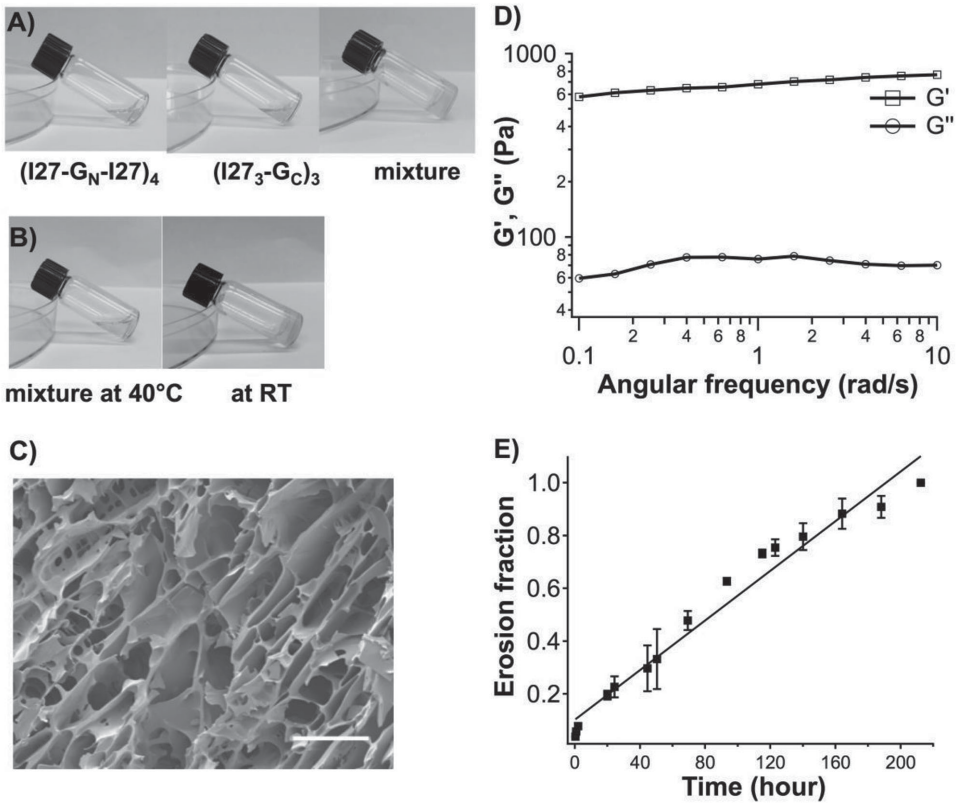


**Figure 3.** Self-assembling protein hydrogels constructed via protein fragment reconstitution. A) Photographs of an aqueous solution of the protein building blocks. A 10% aqueous solution of $(I27\text{-}G_N\text{-}I27)_4$ and $(I27_3\text{-}G_C)_3$ can readily form a hydrogel, while the isolated 10% $(I27\text{-}G_N\text{-}I27)_4$ or 10% $(I27_3\text{-}G_C)_3$ remain solutions. B) Hydrogel formation is temperature dependent, where the 10% hydrogel turns clear at 40 °C (left). Upon cooling to room temperature, the hydrogel reforms (right). C) SEM image of the freeze-dried 10% hydrogel of $(I27\text{-}G_N\text{-}I27)_4$ and $(I27_3\text{-}G_C)_3$ in a reduced state (left) and an oxidized state. The scale bar represents 100 μm. D) The storage modulus G′ and loss modulus G″ of a 10% hydrogel as a function of angular frequency. The storage modulus is ≈700 Pa, which is significantly greater than loss modulus (≈80 Pa). E) The erosion profile of a 100 mg 10% hydrogel containing $(I27\text{-}G_N\text{-}I27)_4$ and $(I27_3\text{-}G_C)_3$, with a surface area of 0.865 $cm^2$ at room temperature. For reduced hydrogel, complete erosion takes about 9 d with an erosion rate of $5.433 \times 10^{-2}$ mg $cm^{-2}$ $h^{-1}$.

modulus G″ (≈80 Pa). G′ remains largely constant from 0.01 to 10 rad $s^{-1}$ at 20 °C, as expected for a stable hydrogel.

Additionally, this hydrogel also shows excellent stability in excess water (Figure 3E). The erosion of the hydrogel shows a linear mass loss versus time profile, suggesting that erosion occurs at the surface of the hydrogel. Despite the physical crosslinking within the hydrogel structure, the erosion rate is very slow; it takes 9 d for the hydrogel to completely erode. This slow erosion of the $(I27\text{-}G_N\text{-}I27)_4/(I27_3\text{-}G_C)_3$ hydrogel compares favorably with that of protein hydrogels constructed from strong protein–protein interactions (such as leucine zipper domains),[9,10,36] suggesting that fragment reconstitution provides a strong driving force for hydrogel formation.

### 2.3. From Physically Crosslinked Hydrogels to Chemically Crosslinked Hydrogels

In addition to the temperature responsiveness of the physically crosslinked hydrogel, this self-assembled protein hydrogel exhibits another unique property: the redox-driven conversion of the physically crosslinked hydrogel to a chemically crosslinked one. The $G_N$ and $G_C$ fragments we used within this study each carry one cysteine residue (Cys41 and Cys43); the location of the two cysteine residues allows for the formation of a disulfide bond in the folded GL5CC form under oxidizing conditions (Figure 1A).[34,37] If this conversion can be accomplished in the hydrogel, the physically crosslinked hydrogel can thus be converted into a chemically crosslinked hydrogel, potentially improving the hydrogel's thermal stability significantly.

To test this hypothesis, we thermally denatured a 1:1 mixture of $G_N$ -I27 and I27-$G_C$. As shown in Figure 2E, the reconstituted $G_N$-$G_C$ has a melting temperature of 22 °C under reduced conditions. After $G_N$ -I27 and I27-$G_C$ reconstituted into a folded domain, we used $H_2O_2$ to oxidize the refolded $G_N$-I27/I27-$G_C$. As shown in **Figure 4**A, two melting transitions are clearly observed in the thermal melting curve of this oxidized sample: the first "unfolding" transition occurs between 10 and 40 °C, which is similar to that of reduced $G_N/G_C$, and the second unfolding transition occurs between 40 and 90 °C, which is similar to that of oxidized GL5CC (Figure S1, Supporting Information). These transitions correspond to a $T_m^1$ of 22 °C and a $T_m^2$ of 63 °C, where the first transition can be ascribed to the melting of reconstituted $G_N/G_C$ in the reduced state, while the second to the melting of the oxidized, reconstituted $G_N/G_C$. This result clearly demonstrates that oxidation can lead to disulfide bond formation within the reconstituted $G_N/G_C$, and that the oxidized $G_N/G_C$ behaves like an intact, native GL5.

Having confirmed the feasibility of oxidizing the reconstituted $G_N/G_C$, we then tested the possibility of converting the $(I27\text{-}G_N\text{-}I27)_4$ and $(I27_3\text{-}G_C)_3$-based physical hydrogel into a chemical hydrogel by oxidation. After forming the hydrogels under reducing conditions, we immersed the hydrogel in phosphate buffered saline (PBS) buffer containing $20 \times 10^{-3}$ M $H_2O_2$ for 30 min. The resultant oxidized hydrogel shows much improved thermal stability: this hydrogel remains a transparent gel even when the temperature is raised to 85 °C (Figure 4B). At temperature higher than 85 °C, the hydrogel remains a gel but turns opaque, an indication that reconstituted $G_N/G_C$ and/or I27 domains in the hydrogel have thermally denatured. This result strongly suggests that following oxidation the hydrogel is converted into a chemically crosslinked hydrogel mediated by the formation of disulfide bond within the reconstituted GL5 domain. SEM imaging shows that the oxidized hydrogel retains a similar porous structure as the reduced hydrogel (Figure 4C).

Rheology measurements show that the storage modulus of oxidized hydrogel increases slightly, from ≈800 to ≈1000 Pa, where the loss modulus remained at 80 Pa (Figure 4D). This result clearly indicates that oxidation does not introduce additional secondary crosslinks, where only physical crosslinks are converted into chemical ones. Thus, the hydrogel structure remains largely unchanged after oxidation, as do viscoelastic properties of the oxidized hydrogels.

The erosion profile of these oxidized hydrogels also demonstrated that they are more stable than reduced ones; for example, reduced hydrogels completely dissolved within 9 days, while ≈50% of the oxidized hydrogels remained after the same amount of time (Figure 4E). This clearly shows that the conversion of physical to chemically crosslinked hydrogels significantly improves their stability in excess water. The erosion profile of the oxidized hydrogel indicates the presence of a sol fraction in the oxidized hydrogel, suggesting that oxidation is not complete. It is of note that the conversion from physically to chemically crosslinked is fully reversible; reducing the hydrogel will revert it back to a physically crosslinked hydrogel. This shows the potential for dynamically tuning the physical/mechanical properties of hydrogel materials in the future.

A similar strategy was developed by Tirrell et al. to enhance the stability of protein hydrogels based on proteins with coiled-coil sequences.[7] By incorporating cysteine residues at specific locations, disulfide bonds can form upon self-association of the coiled coil sequences,[7] leading to improved thermal stability as well as stability against erosion. These results further support that protein engineering can offer additional possibilities for tuning the physical and mechanical properties of hydrogels via the redox potential of their environments.

### 2.4. From Two-Component to Single-Component Hydrogels

The two-component approach described previously offers a convenient way of engineering protein-based hydrogels. In this approach, the two protein fragments must be expressed and purified separately, which could potentially leading to technical challenges. Compared with this two-component approach, a single-component approach could solve many of these technical issues encountered. It could be feasible to use the same protein fragment reconstitution principle to construct protein hydrogels from a single protein component if one could incorporate both $G_N$ and $G_C$ fragments into one protein, and prevent the reconstitution of $G_N/G_C$ via intramolecular fragment reconstitution.

In our previous experiments, we engineered the so-called mutually exclusive protein GL5-I27 (where I27 is inserted into

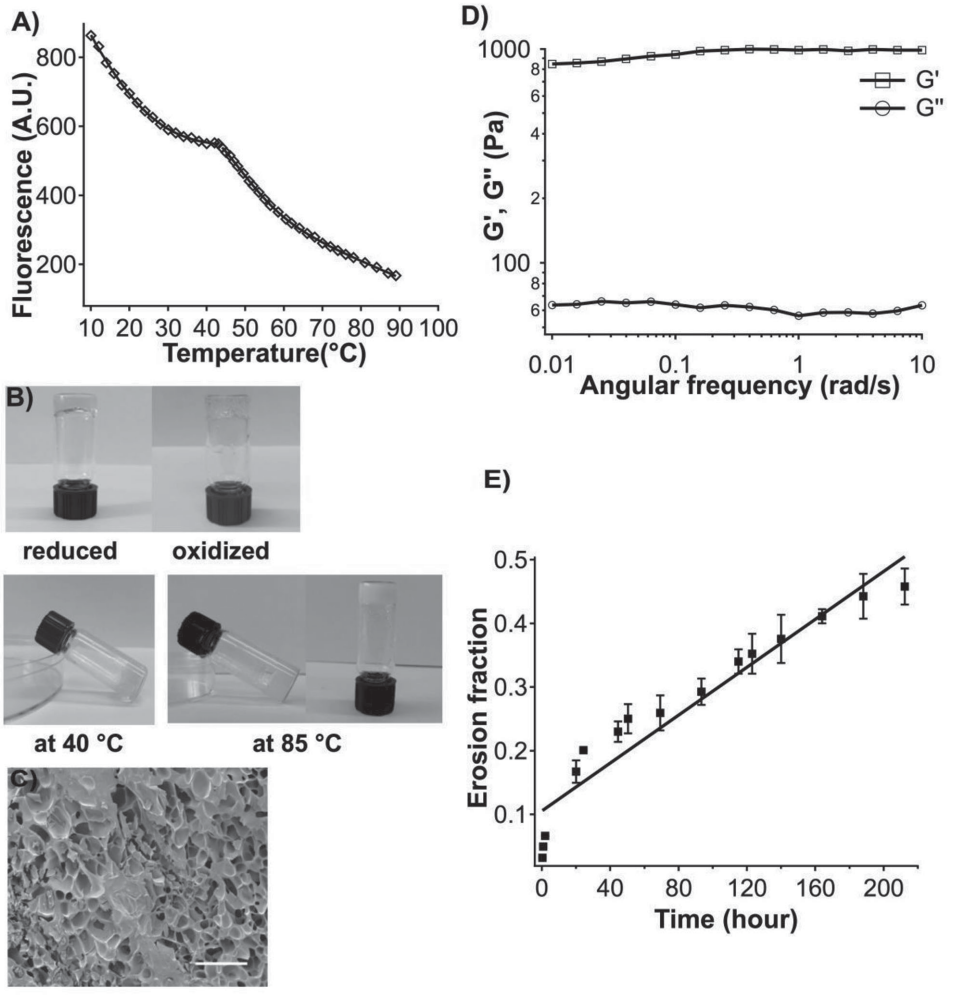


**Figure 4.** The $(I27\text{-}G_N\text{-}I27)_4$ and $(I27_3\text{-}G_C)_3$-hydrogel can chemically crosslinked via the formation of disulfide bonds within the reconstituted $G_N/G_C$-domain. A) Thermal denaturation of the $I27\text{-}G_N$ and $I27\text{-}G_C$ mixture by fluorescence in oxidized states. B) 10% $(I27\text{-}G_N\text{-}I27)_4$ and 10% $(I27_3\text{-}G_C)_3$ hydrogels in the oxidized state show improved thermal stability. Under oxidized conditions ($20 \times 10^{-3}$ M $H_2O_2$), bubbles were observed in the hydrogel due to the production of $O_2$ (top). The oxidized hydrogel remains clear and gelated at 40 °C; however, it turns opaque when temperature is higher than 85 °C. C) SEM image of the 10% $(I27\text{-}G_N\text{-}I27)_4$ and $(I27_3\text{-}G_C)_3$-hydrogel in the oxidized state. D) The storage modulus G′ and loss modulus G″ of the 10% oxidized hydrogel as a function of angular frequency. The storage modulus increases to ≈1000 Pa, comparing to the reduced physical hydrogel (≈700 Pa); the loss modulus remains at ≈80 Pa. E) The oxidized 10% $(I27\text{-}G_N\text{-}I27)_4$ and $(I27_3\text{-}G_C)_3$-hydrogel shows improved stability against erosion. Compared with the reduced hydrogel (which is completely eroded in 9 d (Figure 3E)), 50% of the oxidized hydrogel remains after 9 d, with an erosion rate of $2.173 \times 10^{-2}$ mg cm$^{-2}$ h$^{-1}$.

the loop of the host protein GL5).[33,37] GL5-I27 can be considered as $G_N\text{-}I27\text{-}G_C$; since I27 is thermodynamically more stable than GL5, the thermodynamically stable conformation of GL5-I27 is GL5(U)-I27(F), in which GL5 is unfolded and I27 is folded. Thus, in this mutually exclusive protein GL5-I27 ($G_N\text{-}I27\text{-}G_C$), intramolecular fragment reconstitution is prevented. In our previous work, we constructed chemically crosslinked protein hydrogels using the polyprotein GB1-R-(GB1-GL5CC-I27-R)$_2$,[37] which can be represented as $GR(G\text{-}G_N\text{-}I27\text{-}G_C\text{-}R)_2$. This protein can be considered tetrafunctional in terms of crosslinking, where the fragment reconstitution of $G_N$ and Gc from neighboring molecules can reconstitute the folded GL5 domain via domain swapping. When the protein concentration is sufficiently high, an aqueous solution of $GR(G\text{-}G_N\text{-}I27\text{-}G_C\text{-}R)_2$ should self-assemble to form a physically crosslinked hydrogel (Figure 1C).

Indeed, we found that a 8% (w/w) aqueous solution of $GR(G\text{-}G_N\text{-}I27\text{-}G_C\text{-}R)_2$ can readily form a transparent hydrogel within 30 min. In contrast, a 6% (w/w) aqueous solution of $GR(G\text{-}G_N\text{-}I27\text{-}G_C\text{-}R)_2$ remains a clear viscous solution even after 24 h (**Figure 5**A). As expected, $GR(G\text{-}G_N\text{-}I27\text{-}G_C\text{-}R)_2$-based hydrogelation is temperature dependent; when the temperature is greater than $T_m$, $GR(G\text{-}G_N\text{-}I27\text{-}G_C\text{-}R)_2$-based hydrogels melt into a viscous solution (Figure 5B). Upon cooling, the hydrogel can readily reform, demonstrating the reversible nature of the $GR(G\text{-}G_N\text{-}I27\text{-}G_C\text{-}R)_2$ hydrogel formation. These results are consistent with the physical crosslinking nature of the hydrogel formed via domain-swapping reconstitution.

Figure 5C shows a SEM photograph of a freeze-dried 8% $GR(G\text{-}G_N\text{-}I27\text{-}G_C\text{-}R)_2$ hydrogel. The hydrogel shows a more

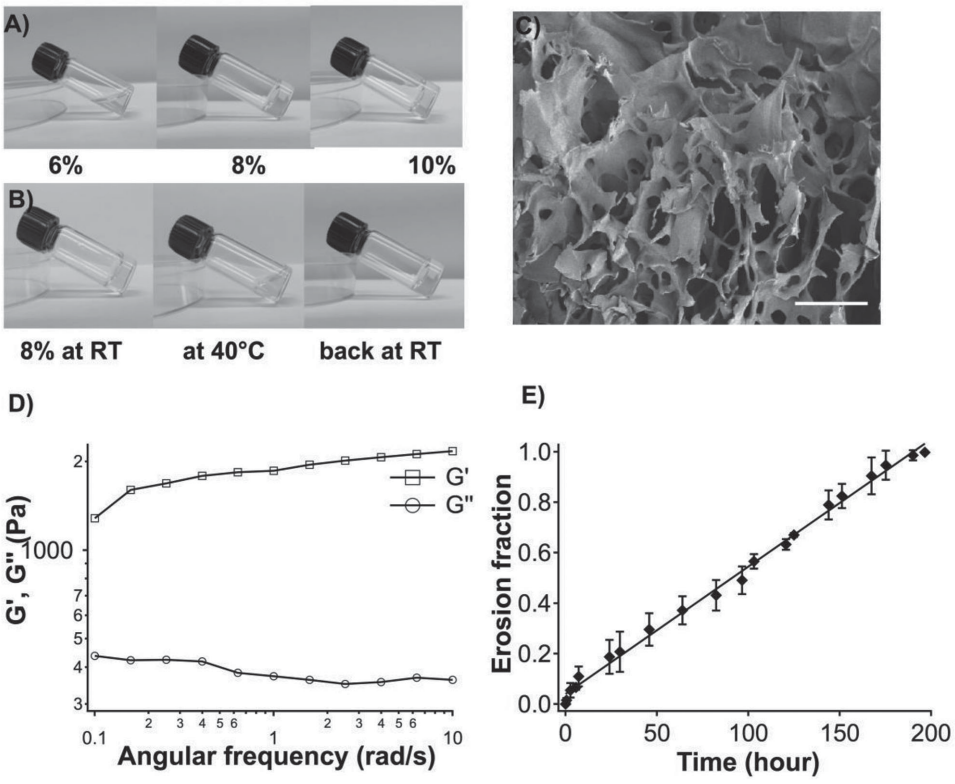


**Figure 5.** A) The GR(G-$G_N$-I27-$G_C$-R)$_2$ aqueous solution can form hydrogels at a concentration as low as 8% (m/v). Photographs of GR(G-$G_N$-I27-$G_C$-R)$_2$ at concentrations ranging from 6% to 10% are shown. B) Hydrogel formation is temperature dependent. The 8% GR(G-$G_N$-I27-$G_C$-R)$_2$ solution forms hydrogel at room temperature, turning to a clear solution at 40 °C. Upon cooling, the hydrogel can readily reform. The scale bar represents 100 μm. C) The storage modulus G′ and loss modulus G″ of the 10% oxidized hydrogel as a function of angular frequency. D) SEM image of the 8% GR(G-$G_N$-I27-$G_C$-R)$_2$ hydrogel. E) The erosion profile of 100 mg 8% hydrogel with a surface area of 0.865 cm$^2$ at room temperature. Complete erosion takes about 10 d, with an erosion rate of $4.74 \times 10^{-2}$ mg cm$^{-2}$ h$^{-1}$.

porous structure than hydrogels made using the two-component approach, with a pore size ranging between tens to 100 μm. This hydrogel has a storage modulus of 800 Pa to 2.3 kPa from 0.01 to 10 rad s$^{-1}$ at 25 °C (Figure 5D).

The hydrogel displays superb stability in excess water and Figure 5E shows its erosion profile. Complete erosion takes ≈10 days, resulting in an erosion rate of $4.74 \times 10^{-2}$ mg cm$^{-2}$ h$^{-1}$. This erosion rate is approximately six times slower than our previously engineered protein hydrogels, which were based on coiled-coil sequence.[9,10] It is likely that the greater degree of physical crosslinking conferred by tetrafunctional polyproteins used to construct these protein hydrogels is responsible for their slow erosion rate.

## 3. Conclusion

Using $G_N$ and $G_C$ proteins as a model system, here we demonstrate that protein fragment reconstitution can be used as a driving force toward engineering protein-based, reversible, self-assembling hydrogels. Based on different protein designs, we constructed protein hydrogels using both two-component as well as single-component designs. These self-assembling protein hydrogels are physical hydrogels in nature and thus show a temperature-dependent sol–gel transition; additionally, they exhibit superb stability against erosion. These properties are comparable to or superb to those reported previously for other protein hydrogels. Given the large number of proteins that can reconstitute into their native fold via fragment reconstitution,[29,38–47] we anticipate that such reconstitution may offer a general driving force for engineering protein hydrogels from a variety of proteins; this will significantly expand the "toolbox" currently available to protein engineers. We anticipate that the concept demonstrated here can be readily implemented in a variety of proteins to construct protein hydrogels with diverse functionalities that are necessary for potential applications in tissue engineering and regenerative medicine. Furthermore, systematic protein engineering efforts will also help tune reconstitution efficiency and binding affinity, thus offering new strategies to tune the mechanical and physical properties of protein hydrogels for a range of applications in biomedical engineering.

## 4. Experimental Section

*Protein Engineering and Hydrogel Preparation*: The polyprotein (I27-$G_N$-I27)$_4$, (I27$_3$-$G_C$)$_3$, and GR(G-$G_N$-I27-$G_C$-R)$_2$ were constructed using standard molecular biology techniques, as previously reported.[37]

The protein $G_N$-I27 and I27-$G_C$ were amplified from GL5CC–I27w34f ($G_N$-I27-$G_C$)[34] via a regular polymerase chain reaction. Plasmids containing desired gene sequences were transformed into the *Escherichia coli* strain DH5$\alpha$. Protein expression was induced using $1 \times 10^{-3}$ M isopropyl-1-$\beta$-D-thiogalactoside. Harvested bacteria culture was centrifuged and lysed using 100 mg $mL^{-1}$ lysozyme and the soluble fraction was purified using a $Co^{2+}$ affinity column. The purified protein was dialyzed against deionized water for 2 d to remove salts, and subsequently lyophilized.

The complete amino acid sequences for GL5CC, $G_N$-I27, I27-$G_C$, (I27-$G_N$-I27)$_4$, (I27$_3$-$G_C$)$_3$, and GR(G-$G_N$-I27-$G_C$-R)$_2$ are detailed in Table S1 (Supporting Information).

Hydrogel was prepared by redissolving the solid protein into $10 \times 10^{-3}$ M dithiolthreitol (DTT)/PBS. To oxidize the hydrogel, the hydrogel was soaked in PBS buffer containing $20 \times 10^{-3}$ M $H_2O_2$ for 30 min. Trapped bubbles were observed in oxidized hydrogel, due to production of $O_2$.

*Stopped-Flow Fluorimetry Measurements*: Stopped-flow experiments were carried out on a BioLogic SFM-4 stopped-flow instrument. Folding and unfolding kinetics of individual I27-$G_C$, individual $G_N$-I27, a 1:1 ratio mixture and intact GL5 were monitored by monitoring the tryptophan fluorescence at 350 nm. The unfolding reaction was initiated and monitored by denaturing a solution of $G_N$-I27 and I27-$G_C$ or GL5 in 4 M GdmCl/$5 \times 10^{-3}$ M DTT/PBS. To investigate the folding kinetics of $G_N$-I27 and I27-$G_C$, folding was initiated and monitored by mixing $G_N$-I27 and I27-$G_C$ with $5 \times 10^{-3}$ M DTT/PBS. To monitor the folding kinetics of GL5, 4 M GdmCl and $5 \times 10^{-3}$ M DTT was initially added to the GL5 solution in order to completely denature the protein. The refolding reaction was initiated by diluting the denatured GL5 from 4 to 0.2 M GdmCl.

*Thermal Denaturation Measurement*: Thermal denaturation experiments were carried out on a Cary Eclipse fluorescence spectrophotometer. Single cell Peltier accessory was used to control temperature. The tryptophan fluorescence at 350 nm was monitored when the temperature was increased from 10 to 90 °C. Raw data were globally fitted using the equation below:

$$f(T) = \frac{(aN + mN \times T) + (aD + mD \times T) \times \exp(m \times (T - Tm)/0.6)}{1 + \exp(m \times (T - Tm)/0.6)}$$

where *aN* is the *y*-intercept of native section, *mN* is the slope of native section, *aD* is the *y*-intercept of denatured section, *mD* is the slope of denatured section, *m* is the slope of transition section, *Tm* is the temperature at which 50% of the protein is denatured.

*Rheology Test*: The viscoelastic response of hydrogel samples was determined by measuring the frequency-dependent viscoelastic moduli $G'(f)$ and $G''(f)$ using a stress-controlled rheometer (HR-2, TA Instruments; New Castle, DE, USA) over a frequency range of three orders of magnitudes. During frequency sweep experiments, deformation was held constant to 1%, with approximately 20 µL sample loaded into the rheometer. Measurements were conducted at room temperature using an 8 mm plate–plate geometry with 250 µm of plate separation. To prevent any drying artifacts, a solvent trap was applied around the sample.

*SEM Imaging*: Each hydrogel was imaged using a Hitachi S4700 scanning electron microscope. An 8% hydrogel sample was prepared in Eppendorf tubes and stored at 4 °C for 24 h to allow the mixture to completely gel. The samples were then shock-frozen in liquid nitrogen and quickly transferred to a freeze drier where they were lyophilized for 12 h. Dry samples were then carefully fractured in liquid nitrogen and fixed on aluminum stubs. The sample surface was coated by 5 nm of gold prior to SEM measurements.

*Erosion Rate Measurements*: The hydrogel erosion rate was measured using previously reported methods.[10] Briefly, 8 mg of GR(G-$G_N$-I27-$G_C$-R)$_2$ protein was dissolved in 100 µL PBS buffer to a concentration of 8%. These protein solutions were then transferred to a cylindrical glass tube with a flat bottom (1.05 cm diameter) and the hydrogel allowed to stand overnight. The hydrogel was then soaked in 2 mL of PBS, and placed on a compact rocker mechanism rotating at 50 rpm. Erosion profiles were determined by measuring the protein content of the supernatant using the absorbance at 280 nm at successive time points using a Nanodrop ultraviolet-visible spectrophotometer; two hydrogel samples were measured and the average values were reported.

## Supporting Information

Supporting Information is available from the Wiley Online Library or from the author.

## Acknowledgements

The work was supported by Canadian Institutes of Health Research and Canada Research Chairs program.

Received: June 4, 2015
Revised: July 6, 2015
Published online: August 4, 2015

[1] R. Langer, D. A. Tirrell, *Nature* **2004**, *428*, 487.
[2] M. P. Lutolf, J. A. Hubbell, *Nat. Biotechnol.* **2005**, *23*, 47.
[3] J. Kopecek, J. Yang, *Angew. Chem. Int. Ed. Engl.* **2012**, *51*, 7396.
[4] S. Banta, I. R. Wheeldon, M. Blenner, in *Annual Review of Biomedical Engineering*, Vol.12, Eds.: M. L. Yarmush, J. S. Duncan, M. L. Gray), Annual Reviews, Palo Alto, CA, USA **2010**, pp. 167–186.
[5] R. L. DiMarco, S. C. Heilshorn, *Adv. Mater.* **2012**, *24*, 3923.
[6] W. A. Petka, J. L. Harden, K. P. McGrath, D. Wirtz, D. A. Tirrell, *Science* **1998**, *281*, 389.
[7] W. Shen, R. G. H. Lammertink, J. K. Sakata, J. A. Kornfield, D. A. Tirrell, *Macromolecules* **2005**, *38*, 3909.
[8] M. M. Stevens, S. Allen, M. C. Davies, C. J. Roberts, J. K. Sakata, S. J. B. Tendler, D. A. Tirrell, P. M. Williams, *Biomacromolecules* **2005**, *6*, 1266.
[9] Y. Cao, H. Li, *Chem. Commun.* **2008**, 4144.
[10] S. Lv, Y. Cao, H. Li, *Langmuir* **2012**, *28*, 2269.
[11] H. D. Lu, I. R. Wheeldon, S. Banta, *Protein Eng. Des. Sel.* **2010**, *23*, 559.
[12] I. R. Wheeldon, S. C. Barton, S. Banta, *Biomacromolecules* **2007**, *8*, 2990.
[13] I. R. Wheeldon, E. Campbell, S. Banta, *J. Mol. Biol.* **2009**, *392*, 129.
[14] I. R. Wheeldon, J. W. Gallaway, S. C. Barton, S. Banta, *Proc. Natl. Acad. Sci. USA* **2008**, *105*, 15275.
[15] N. Yamaguchi, L. Zhang, B. S. Chae, C. S. Palla, E. M. Furst, K. L. Kiick, *J. Am. Chem. Soc.* **2007**, *129*, 3040.
[16] H. D. Lu, M. B. Charati, I. L. Kim, J. A. Burdick, *Biomaterials* **2012**, *33*, 2145.
[17] H. D. Lu, D. E. Soranno, C. B. Rodell, I. L. Kim, J. A. Burdick, *Adv. Healthcare Mater.* **2013**, *2*, 1028.
[18] C. Foo, J. S. Lee, W. Mulyasasmita, A. Parisi-Amon, S. C. Heilshorn, *Proc. Natl. Acad. Sci. USA* **2009**, *106*, 22067.
[19] A. Galarneau, M. Primeau, L. E. Trudeau, S. W. Michnick, *Nat. Biotechnol.* **2002**, *20*, 619.
[20] J. Jeong, S. K. Kim, J. Ahn, K. Park, E. J. Jeong, M. Kim, B. H. Chung, *Biochem. Biophys. Res. Commun.* **2006**, *339*, 647.
[21] D. D. Ojennus, S. E. Lehto, D. S. Wuttke, *Protein Sci.* **2003**, *12*, 44.
[22] F. Rossi, C. A. Charlton, H. M. Blau, *Proc. Natl. Acad. Sci. USA* **1997**, *94*, 8405.

[23] T. K. Kerppola, *Chem. Soc. Rev.* **2009**, *38*, 2876.
[24] S. W. Michnick, P. H. Ear, E. N. Manderson, I. Remy, E. Stefan, *Nat. Rev. Drug Discovery* **2007**, *6*, 569.
[25] M. C. Bauer, W.-F. Xue, S. Linse, *Int. J. Mol. Sci.* **2009**, *10*, 1552.
[26] N. Kobayashi, S. Honda, E. Munekata, *Biochemistry* **1999**, *38*, 3228.
[27] S. Honda, N. Kobayashi, E. Munekata, H. Uedaira, *Biochemistry* **1999**, *38*, 1203.
[28] N. Kobayashi, S. Honda, H. Yoshii, H. Uedaira, E. Munekata, *FEBS Lett.* **1995**, *366*, 99.
[29] N. Johnsson, A. Varshavsky, *Proc. Natl. Acad. Sci. USA* **1994**, *91*, 10340.
[30] J. N. Pelletier, F. X. Campbell-Valois, S. W. Michnick, *Proc. Natl. Acad. Sci. USA* **1998**, *95*, 12141.
[31] A. G. Ladurner, L. S. Itzhaki, G. D. Gay, A. R. Fersht, *J. Mol. Biol.* **1997**, *273*, 317.
[32] E. L. McCallister, E. Alm, D. Baker, *Nat. Struct. Biol.* **2000**, *7*, 669.
[33] Q. Peng, H. Li, *J. Am. Chem. Soc.* **2009**, *131*, 13347.
[34] Q. Peng, N. Kong, H. C. E. Wang, H. B. Li, *Protein Sci.* **2012**, *21*, 1222.
[35] S. S. Lv, T. J. Bu, J. Kayser, A. Bausch, H. B. Li, *Acta Biomater.* **2013**, *9*, 6481.
[36] W. Shen, K. C. Zhang, J. A. Kornfield, D. A. Tirrell, *Nat. Mater.* **2006**, *5*, 153.
[37] N. Kong, Q. Peng, H. Li, *Adv. Funct. Mater.* **2014**, *24*, 7310.
[38] T. Berggard, K. Julenius, A. Ogard, T. Drakenberg, S. Linse, *Biochemistry* **2001**, *40*, 1257.
[39] A. Holmgren, *FEBS Lett.* **1972**, *24*, 351.
[40] G. D. Gay, J. Ruizsanz, B. Davis, A. R. Fersht, *Proc. Natl. Acad. Sci. USA* **1994**, *91*, 10943.
[41] R. R. Hantgan, H. Taniuchi, *J. Biol. Chem.* **1977**, *252*, 1367.
[42] L. Stewart, G. C. Ireton, J. J. Champoux, *J. Mol. Biol.* **1997**, *269*, 355.
[43] M. L. Tasayco, K. Chao, *Proteins: Struct. Funct. Genet.* **1995**, *22*, 41.
[44] V. F. Smith, C. R. Matthews, *Protein Sci.* **2001**, *10*, 116.
[45] W. F. Xue, J. Carey, S. Linse, *Proteins: Struct. Funct. Bioinf.* **2004**, *57*, 586.
[46] J. Carey, S. Lindman, M. Bauer, S. Linse, *Protein Sci.* **2007**, *16*, 2317.
[47] S. Linse, E. Thulin, L. K. Gifford, D. Radzewsky, J. Hagan, R. R. Wilk, K. S. Akerfeldt, *Protein Sci.* **1997**, *6*, 2385.